Journal of The Electrochemical Society, **159** (11) C441-C446 (2012)
0013-4651/2012/159(11)/C441/6/$28.00 © The Electrochemical Society

Improvement in Coating Quality and Corrosion Characteristics of Galvanized Steels by Pre-Electrodeposition of Cu

Yun-Il Choi,[a] Doojin Paik,[b] Masazumi Okido,[c] Kensuke Kuroda,[c] and Chan-Jin Park[d,*,z]

[a]*Department of Materials Science and Engineering, Graduate School of Engineering, Nagoya University, Nagoya 464-8603, Japan*
[b]*Surface Treatment Department, POSCO, Gwangyang, Jeonnam 545-090, Korea*
[c]*EcoTopia Science Institute, Nagoya University, Nagoya 464-8603, Japan*
[d]*Department of Materials Science and Engineering, Chonnam National University, Gwangju 500-757, Korea*

A dual-phase steel was electrodeposited with Cu prior to reduction annealing in order to improve coating quality and resultant corrosion characteristics of the galvanized material. This pre-eletrodeposition process allowed a tenfold reduction in coating defects (typically found in uncoated areas and empty pores), thereby yielding a 8.4% coating weight gain and a noticeable decrease (24%) in the average spangle diameter. However, the Cu pre-electrodeposition layer acted as an inter-diffusion barrier, thereby limiting Fe-Al interactions during galvanization, and resulted in the formation of imperfect Fe-Al compounds. Nevertheless, this Cu layer could extend the incubation time of the Fe-Zn phases. Consequently, the presence of this Cu electrodeposition layer could effectively prevent concentration polarization, thereby decreasing corrosion current density even after 4 days of immersion in 3.5% NaCl solution.

Manuscript submitted June 7, 2012; revised manuscript received July 30, 2012. Published August 31, 2012.

Among the large variety of metals used for steel coating, Zn has been found to provide superior barrier and galvanic protection upon exposure corrosive environments. These Zn coatings are typically manufactured in continuous hot-dip galvanizing production lines forming automotive body panels. During the galvanizing, the molten Al atoms (0.1–0.3 mass% Al is generally added to a molten Zn pot) interact with the Fe atoms in the solid state, developing very thin and ductile Fe-Al intermetallic phases without loss of coating adhesion to the steel substrate.[1] However, if the metallurgical linkages between the steel substrate and the molten Al become weak, the composition of the bonding zone might change, and consequently, coating defects in the final galvanized steels, the so-called "outburst" would be formed. The Fe-Al intermetallic phases at the coating/substrate interface act as an inhibition layer, thereby slowing down the Fe-Zn inter-diffusion. Furthermore, although the Fe-Zn intermetallic phases can provide a high bonding strength between the Zn coating and the steel substrate,[2,3] these phases are typically very brittle and thick, leading to the onset of disbond cracks in the galvanized coatings during the galvanization process.[4–8] Consequently, careful control over the formation of Fe-Zn intermetallic phases is required in the galvanized steels.

The subsequent reduction annealing process, typically carried out under a $H_2 + N_2$ atmosphere with a dew point of -30°C, can also lead to structural issues in galvanized steels.[9,10] Thus, minor alloying elements such as Si, Mn, and Al (normally found in advanced high-strength steels) segregate to the surface, causing a high degree of external oxidation. A large amount of studies corroborated that the extent of this selective surface oxidation depends on the dew point of the reducing atmosphere and the nature of the corresponding oxides formed.[11–17] These external concentrated oxides have low wettability with molten Zn, and hence, the formation of surface defects such as outbursts in galvanized coatings is triggered.[18,19] Furthermore, these surface defects can serve as preferential sites for corrosive attack upon exposure of the sheets to environment conditions. A potential solution to reduce the extent of surface oxidation involves utilization of reducing atmospheres with lower dew point temperatures. However, this would obligate steel manufacturers to continuously adapt the dew point temperature to the various types of steel sheets passing through the annealing line on a daily basis,[20] which is realistically impossible. In this sense, new strategies to avoid the selective surface oxidation under reducing atmospheres with a relatively high dew point temperature are needed. Improvement of the surface quality and the associated corrosion resistance of galvanized coatings have been studied extensively in the past years. Tobiyama et al.[21] reported that the surface defects on galvanized coatings can be effectively suppressed by electrodepositing Fe (0.1–10 g m^{-2}) on the steel sheets prior to reduction annealing. Similarly, Sakurai et al. demonstrated a notable reduction in the concentration of coating defects by electrodepositing a 0.01–3.0-μm-thick layer of pure metal or alloys containing Fe, Ni, Co, and Cu on the pre-annealed steel sheets before dipping them into the Zn pot.[22] Recently, Sa-nguanmoo et al. applied pulsed current waveforms to pre-electrodeposit Ni over the steel sheets.[23] Shibli and Maru reported the beneficial effects of electrolessly deposited Ni on the growth of intermediate layer and the corrosion resistance of galvanized coatings.[24] Corrosion resistance can be alternatively improved by application of post-treatments to ordinary galvanized coatings such as conversion coating, phosphating, and oxide deposition.[25–28] We recently demonstrated that formation of Mn and Si oxides on the surface of a dual-phase steel can be effectively suppressed during reduction annealing by pre-electrodepositing Cu or Fe.[29,30] The amount of electrodeposits on the steel sheets ranged from 0.2 to 0.4 g m^{-2}, corresponding to a thickness of 22–50 nm, was enough to significantly reduce the surface defects on the final galvanized coatings.

In the present study, we investigated, in a more systematic manner, the influence of Cu pre-electrodeposits prior to reduction annealing on the surface quality and resultant corrosion characteristics of galvanized dual-phase steels.

Experimental

The chemical composition of the dual-phase steel used as a substrate was Mn 1.0, Si 0.31, Al 0.053, C 0.088, P 0.01, S 0.006, and Fe balance (mass%). The steel sheets were first degreased with ethanol and acetone, cathodically cleaned at 100 mA cm^{-2} for 5 min in a 10 mass% NaOH solution, activated in a 10% HCl solution, and finally neutralized with deionized water. The samples were then masked with polypropylene tape, leaving an exposed area of 55 cm^2.[29] Cu was galvanostatically electrodeposited over the steel sheets for only 1 s at 120 mA cm^{-2} in a bath containing 0.8 M $CuSO_4.5H_2O$ + 0.4 M H_2SO_4 at 25°C. The corresponding electrodeposition potential was $-0.1\ V_{SCE}$ and the amount of Cu electrodeposited was approximately 0.2–0.4 g m^{-2}. Following electrodeposition, reduction annealing was carried out at 800°C for approximately 1 min in a reducing atmosphere of 15% H_2 in N_2 (v/v) with a dew point of -30°C. The steel sheets were then dipped into a molten Zn pot containing a maximum of 0.3 mass% Al. After withdrawing the sheets from the molten Zn pot, the amount of liquid Zn was controlled to 3.8–4.0 mg cm^{-2}, and the sheets were finally quenched. These processes were carried out using a laboratory-scale galvanizing simulator.

*Electrochemical Society Active Member.
zE-mail: parkcj@chonnam.ac.kr

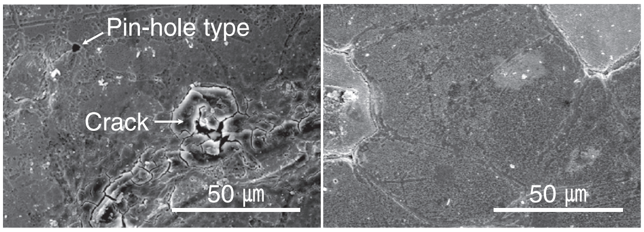

(a) (b)

Figure 1. Surface morphologies of the galvanized steels; (a) conventional, (b) Cu pre-electrodeposited.

The microstructure and corresponding chemical composition of galvanized coatings were analyzed by optical microscopy (OM), scanning electron microscopy (SEM), and energy-dispersive spectrometry (EDS). In order to determine the average spangle diameter, a 3-mm-long line was drawn across the micrographs, and the number of spangle boundary intercepts, n, was subsequently counted. The spangle size, d, was then determined by the following equation: $d = 3/n$. The area fraction of coating defects was determined by a quantitative image analyzer by recording 12 consecutive micrographs with the same focus range ($\times 50$). The area fraction with coating defects was defined as the ratio of the defect area to the total area.

The corrosion characteristics of galvanized steels were assessed by electrochemical impedance spectroscopy (EIS) and then anodic polarization tests after 1 h and 4 days of immersion in a deaerated 3.5 mass% NaCl aqueous solution at 25°C. To prevent edge corrosion, the edge and back parts of the samples were masked with silicone paste. In the EIS measurements, the real and imaginary parts of the electrochemical cell were assessed over a nominal frequency range set to 10^4 Hz to 10^{-2} Hz with a 10 mV amplitude, where the applied potential was an open-circuit potential (E_{OCP}). Measurement for the anodic polarization tests were then carried out with a scan rate set to 0.5 mV s^{-1}. All the electrochemical measurements were carried out after stabilizing E_{OCP} in a three-electrode system. The galvanized steels under study served as the working electrode (WE); a 0.8-mm-thick platinum wire was used as the counter electrode (CE); while a saturated calomel reference electrode (Hg/Hg_2Cl_2/sat.KCl) with a Luggin probe acted as the reference electrode (RE). All experiments were repeated three times, and the obtained results were reproducible.

Results and Discussion

Effects on coating quality.— As shown in Figs. 1 and 2, two types of surface defects, i.e. cracks and pin-holes, were primarily found on conventional galvanized coatings. These cracks and pin-holes resulted from Si- and Mn-containing oxides, respectively, during reduction annealing prior to galvanization.[29] Minor alloying elements in dual-phase steels oxidize because of their lower standard Gibbs free energy change (ΔG°) as compared to that of Fe oxidation reaction under reduction annealing conditions. These oxide compounds, especially the amorphous Si or Si/Mn complex oxides, are in a condensed state, thereby hindering the wetting characteristics of the steel substrate and inducing many defects in final galvanized coatings (see Figs. 1a and 2a).

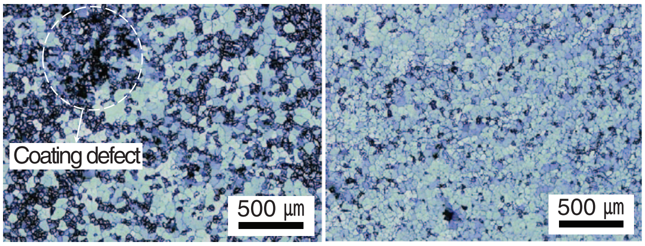

(a) (b)

Figure 2. Optical micrographs of the galvanized coatings; (a) conventional, (b) Cu pre-electrodeposited.

Table I. The average spangle size in diameter (μm), area fraction of coating defects, and coating mass (g m^{-2}) of conventional and Cu pre-electrodeposited galvanized steels (σ: standard deviation).

	Conventional	Cu pre-electrodeposited
Average spangle diameter (μm)	63.1 ($\sigma = 24.8$)	50.5 ($\sigma = 7.2$)
Average area fraction of coating defects	0.067 ($\sigma = 0.006$)	0.005 ($\sigma = 0.001$)
Average coating mass (g m^{-2})	40.9 ($\sigma = 2.1$)	48.6 ($\sigma = 3.0$)

Remarkably, these unwanted coating defects were significantly reduced (more than tenfold) by pre-electrodepositing Cu prior to reduction annealing, as shown in Table I. The slow kinetics of formation of amorphous-Si-containing oxides under a particular reduction annealing atmosphere, which can be attributed to electrodeposition, has been previously proposed to explain this beneficial effect.[29] The strong reduction in the concentration of coating defects with the applied electrodeposition current intensity supports this hypothesis. It is known that the nucleation and growth rate of Cu particles during the electrodeposition are mainly influenced by the applied cathodic overvoltage. However, good control over the electrodeposition process is crucial to avoid imperfect overlay of the steel substrate which may leads to rapid oxidation of Si, Mn, and even Fe by Cu during the reduction annealing. The probability of these unwanted oxidation processes to occur increases with the difference of ΔG° between the two metals. With these aspects in mind, a high cathodic overvoltage corresponding to a current density of 120 mA cm^{-2} was applied to obtain fine Cu electrodeposits with a high nucleation density. This current density was found to be optimum to effectively decrease the degree of selective surface oxidation during the reduction annealing while reducing the coating defects after the galvanization process.[29] As a result, the coating mass of the galvanized steel was increased by about 19% (from 40.9 to 48.6 g m^{-2}, Table I). As shown in Figs. 3a and 3b, ordinary coating methods based on unwanted Fe-Zn interdiffusion typically led to the formation of surface cracks and a large number of empty pores. The pre-electrodeposition of Cu, on the other hand, generated a coating layer with a higher thickness, which accounts for the higher coating weight observed (Table I). This parameter is important in that the service life of galvanized steel is a direct function of its coating weight (90 g m^{-2} $\approx$ 20–25 years).[31]

As shown in Table I, the average spangle size on galvanized coating was decreased by about 24% (from 63.1 to 50.5 μm in diameter). The spangle size is known to be mainly affected by the cooling conditions during crystallization (e.g., solidification). Thus, it is known that quenching with water can decrease the spangle size and prevent any Fe-Zn intermetallic phase from formation. The above results suggest that the Cu electrodeposition itself is able to reduce the spangle size probably by increasing the nucleation sites at the substrate/liquid Zn interface. Thus, the presence of Cu electrodeposits on the steel substrate could increase the solid/liquid interfacial energy in the solidifying Zn coatings, thereby increasing in growth velocity of new spangles. Reduction in the spangle size became more prominent as the electrodeposition current density increased (6 mA cm^{-2}: about 16%, 120 mA cm^{-2}: about 24%). This phenomenon is worthy of notice in that the decrease in spangle size can enhance the adhesion strength of organic paint to the galvanized coating.[32]

As shown in Fig. 4, the pre-electrodeposited thin Cu layer inherent to the steel substrate completely disappeared after galvanization. This unexpected phenomenon was consistent with the in-depth profile results obtained by glow discharge spectrometry (GDS, results not shown) and seems to be explained by high diffusion ability of Cu upon galvanization at 450°C. According to an equilibrium phase diagram

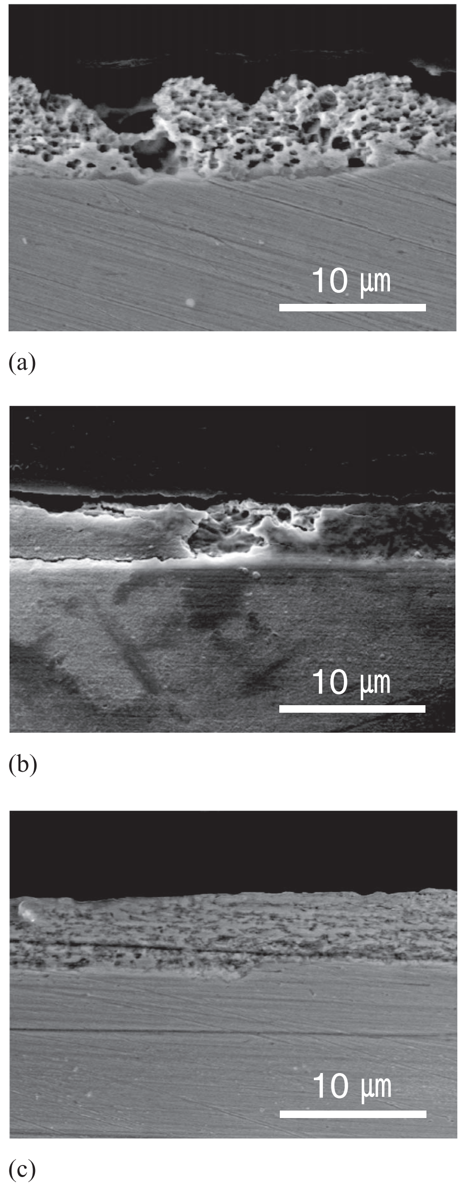

Figure 3. Cross sections of the galvanized coatings; (a), (b) defect-containing coating areas, (c) ordinary coating area. Conventional galvanized coating led to a number of surface defects comprised of a large number of empty pores and uncoated areas. These coating defects were reduced by approximately tenfold after pre-electrodepositing Cu prior to reduction annealing.

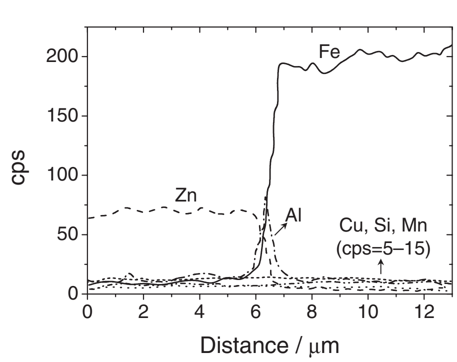

Figure 4. Energy dispersive spectrometer (EDS) line-scan profile of the galvanized steel pre-electrodeposited with Cu.

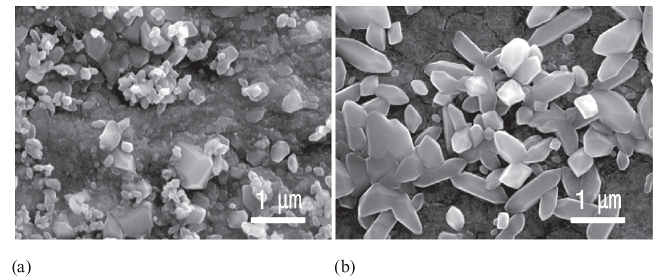

Figure 5. Surface morphologies of the Fe-Al compounds formed at the coating/substrate interface; (a) conventional, (b) Cu pre-electrodeposited.

of Zn-Cu, Zn containing 0–2.83 mol% Cu exists in the liquid state at temperatures higher than 420°C, leading to the highly significant diffusion of the Cu into the galvanized coating during solidification. Several alternative elements such as Ni and Co also may be rapidly diffused upon the galvanization because they exist in the liquid states on Zn-rich sides of each equilibrium phase diagram at 450°C. During the solidification, the Cu electrodeposits placed between liquid Zn and steel substrate, unfortunately, acted as a diffusion barrier, thereby retarding the reactive inter-diffusion between Fe and Al, as shown in Fig. 5 and Table II. The development of a continuous layer of Fe-Al at the coating/substrate interface is important in that it temporary inhibits the so-called "outburst reaction", which refers to the formation of Fe-Zn intermetallic phases at substrate grain boundaries.[4–6] The brittle Fe-Zn intermetallic phases are responsible for volume expansion, breaking the inhibitive Fe-Al compounds, and ultimately inducing the onset of coating defects in galvanized steels. The Cu electrodeposits retarded the Al uptake process at the coating/substrate interface during the galvanization, thereby limiting the nucleation and growth of Fe-Al compounds and resulting in the incomplete development of pancake-shaped Fe-Al compounds, as shown in Fig. 5b. Several researchers have described the formation of Fe-Al compounds by a two-stage growth mechanism: (i) an initial formation of compact, lower layer (comprised of close-packed crystals) adjacent to the substrate by rapid interface controlled reaction, and (ii) subsequent formation of a thick upper layer with pancake-shaped crystals by solid-state diffusion of Fe.[33,34] Cu electrodeposits itself could, however, increase the incubation time, i.e. the time required for the formation of Fe-Zn intermetallic phases during the galvanization, instead of or along with the incompletely formed Fe-Al compounds, resulting in the reduction in the coating defects. Furthermore, the presence of novel elements such as Cu in the coating as a result of diffusion processes during galvanization may improve the mechanical and electrochemical characteristics of galvanized steels. However, electrodeposition of novel metals less than 0.5 g m^{-2} is recommended to avoid an excessive increase in the weight of the vehicle.

Effects on corrosion characteristics.— EIS measurements were carried out to examine the accurate mechanistic information and charge-transfer kinetics across the galvanized coating layer-steel substrate interface. The obtained impedance plots revealed different time-constants with immersion time. Therefore, proper equivalent circuit architectures were applied to each electrochemical system, as shown in Fig. 6. A constant phase element (CPE) was used to compensate the deviations from the ideal dielectric behavior as a result of a depressed

Table II. Chemical composition of inhibition layers formed at the coating/substrate interface of conventional and Cu pre-electrodeposited galvanized steels depicted in Fig. 5.

	Al	Si	Mn	Fe	Zn
Conventional	22.02	0.44	1.37	73.59	2.58
Cu pre-electrodeposited	16.17	0.33	1.24	81.26	1.00

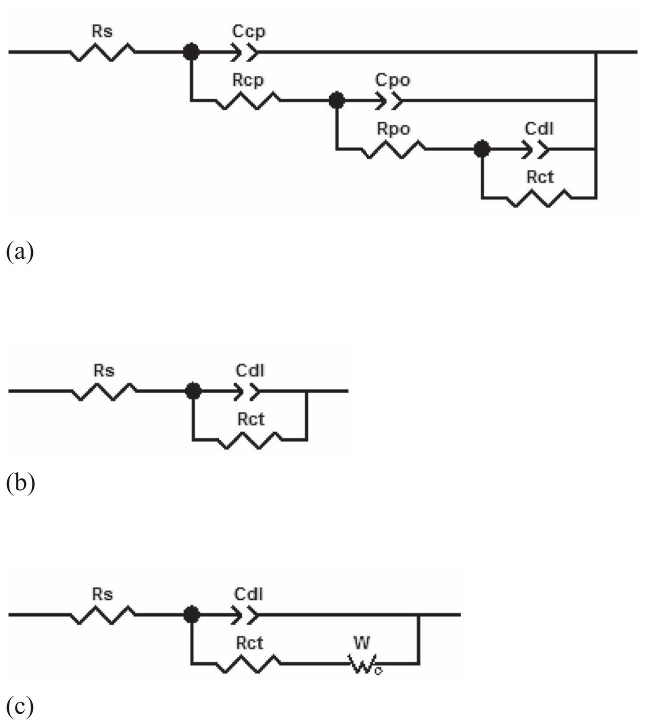

Figure 6. Equivalent circuits used to examine the parameters in electrochemical impedance plots in Figs. 7 and 8; (a) both samples (after 1 h), (b) Cu pre-electrodeposited (after 4 days), and (c) conventional (after 4 days).

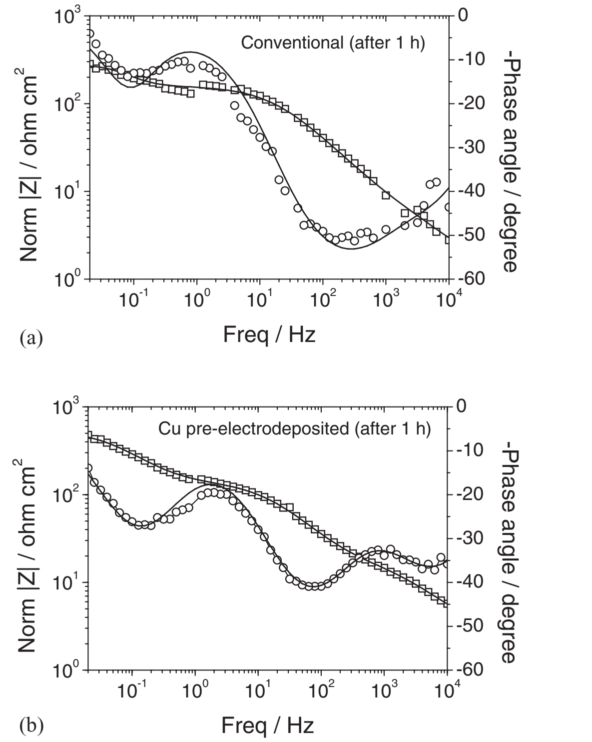

Figure 7. Electrochemical impedance plots of the conventional galvanized steels measured in a deaerated 3.5 mass% NaCl solution at 25°C; after immersion for (a) 1 h, (b) 4 days.

semicircle in Nyquist plots. R_s is the solution resistance between the reference electrode tip and the galvanized coating surface, R_{cp} is the corrosion product resistance representing the resistance of Zn-based corrosion products mainly deposited in the defects of galvanized coating upon immersion, R_{po} is the coating resistance (pore resistance) representing the resistance of galvanized coating which is associated with the electrolyte penetration into its defects and pores, and R_{ct} refers to the charge transfer resistance representing the resistance at an interface of galvanized coating/substrate where corrosion occurs. C_{cp} implies the capacitance of corrosion products primarily deposited in the defects of galvanized coating upon immersion, C_{po} represents the capacitance of galvanized coating associated with the electrolyte penetration through the coating defects and pores, C_{dl} indicates the double layer capacitance at an area beneath the galvanized coating where corrosion occurs, and W is the Warburg impedance representing the diffusion process of corrosive ions (such as Cl^-) from the electrolyte solution.

As shown in Fig. 7, all Bode plots were characterized by three different time-constants after 1 h of immersion in 3.5% NaCl, indicating that the equivalent circuit models for these electrolyte/coating/substrate cells were composed with three resistive components. The existence of a third time-constant at a high frequency (> 10^3 Hz) is attributed to the Zn-based corrosion products initially generated and accumulated in the coating defects of galvanized steel upon the exposure environment. In this context, a threefold higher R_{cp} of conventional galvanized coating (53.8 Ω cm^2) as compared to Cu pre-electrodeposited part (18.9 Ω cm^2) signifies that this coating layer is ineffective to protect the substrate against the corrosion, resulting from the high corrosion rate (i_{corr} = 40.3 μA cm^{-2}, Table III). On the other hand, for the Cu pre-electrodeposited steel, the relatively lower value of R_{cp} (18.9 Ω cm^2) in comparison to those of R_{ct} (460.3 Ω cm^2) and R_{po} (121.2 Ω cm^2) indicates that the effect of corrosion products on the overall corrosion resistance of galvanized steel is negligible during 1 h of immersion, which accounts for the high corrosion-resistant galvanized coating resulting from the dense and compact coating layer observed. The presence of a second time-constant at a middle frequency (10^1–10^3 Hz) is distinctly due to the porous galvanized coatings (Fig. 7). Thus, the higher R_{po} of Cu pre-electrodeposited galvanized steel as compared to conventional galvanized steel after 1 h of immersion indicates that the steel substrate was fully covered by the galvanized coating, thereby resulting in a fourfold increase in R_{ct}, as shown in Table III.

However, the one time-constant which is associated with the formation of thick and protective Zn hydroxide layer on the galvanized coating contributed to the corrosion process after 4 days of immersion (Fig. 8). The Cu pre-electrodeposited galvanized steel afforded a higher R_{ct} (by about 3 times) as compared to the conventional part as a result of an effective filling and blockage of coating defects by the Zn hydroxide. However, the corrosion process of the conventional part was controlled by the concentration polarization of corrosive species (Warburg impedance) after 4 days of immersion, thereby showing that

Table III. Charge transfer resistance R_{ct}, pore resistance R_{po}, corrosion product resistance R_{cp}, Corrosion potential E_{corr}, and corrosion current density i_{corr} of galvanized steels determined from the impedance plots in Figs. 7 and 8 and potentiodynamic curves in Fig. 9.

		E_{corr} (mV$_{SCE}$)	i_{corr} (μA cm^{-2})	R_{ct} (Ω cm^2)	R_{po} (Ω cm^2)	R_{cp} (Ω cm^2)	W (mS s$^{1/2}$ cm^{-2})
Conventional	1 h	−1.14	40.3	101.1	103.7	53.8	-
	4 days	−1.32	141.8	174.7	-	-	31.7
Cu pre-electrodeposited	1 h	−0.98	9.4	460.3	121.2	18.9	-
	4 days	−1.26	18.3	613.1	-	-	-

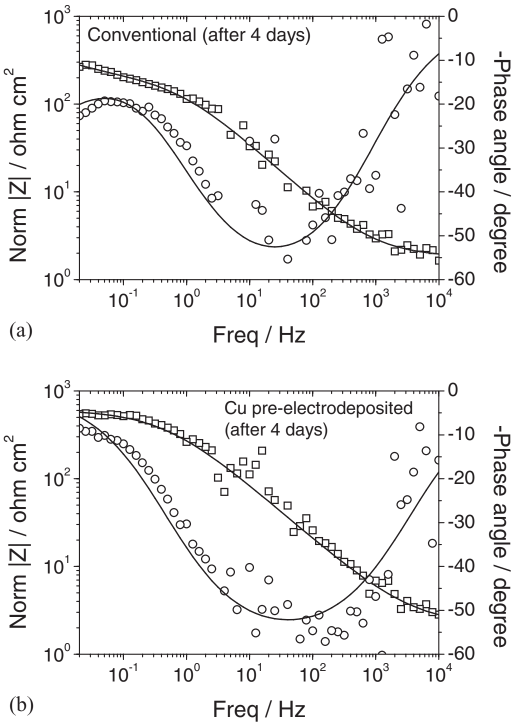

Figure 8. Electrochemical impedance plots of the Cu pre-electrodeposited galvanized steels measured in a deaerated 3.5 mass% NaCl solution at 25°C; after immersion for (a) 1 h, (b) 4 days.

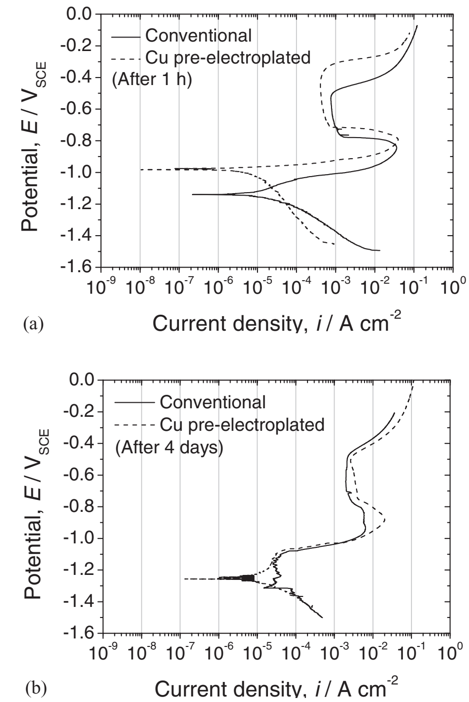

Figure 9. Potentiodynamic curves of the galvanized steels measured in a deaerated 3.5 mass% NaCl solution at 25°C; after immersion for (a) 1 h, (b) 4 days.

this material cannot effectively prevent the mass diffusion from the electrolyte to the Zn hydroxide layer. The mass diffusion of corrosive species adjacent to the electrode surface refers to the diffusive transport resulting from concentration gradients and controls the corrosion rate according to the first Fick's law ($J = -D(\partial C/\partial x)$).[35] Therefore, the extent of this diffusion process depends on the stability and homogeneity of galvanized coating layer, and consequently, it offers the indication of the fraction of coating defects. In this sense, a tenfold lower fraction of the coating defects of Cu pre-electrodeposited galvanized coating led to a threefold higher polarization resistance R_p (i.e. the sum of all resistances) even after 4 days of immersion.

The anodic polarization behavior of Cu pre-electrodeposited galvanized steel was investigated and compared with that of a conventional material after 1 h and 4 days of immersion. As shown in Fig. 9a, the galvanized coating pre-electrodeposited with Cu exhibited a higher corrosion potential E_{corr} (-0.98 V_{SCE}) and lower corrosion current density i_{corr} (9.4 $\mu A\ cm^{-2}$) than those of the conventional part ($E_{corr} = -1.14$ V_{SCE}, $i_{corr} = 40.3$ $\mu A\ cm^{-2}$) after 1 h of immersion, and resulted in lower anodic currents at potentials near the OCP. Furthermore, the pre-electrodeposition of Cu afforded a typical anodic polarization behavior of galvanized coatings, i.e. a highly depolarized anodic reaction,[36] whereas a passive state emerged at -1.1–1.0 V_{SCE} for the conventional galvanized coating. These phenomena can be explained in base of a rapid precipitation of corrosion products such as $Zn(OH)_2$ over the galvanized coating during the first 1 h of immersion, which results from the high corrosion rate observed for this material. These results are consistent with those of EIS analysis that the conventional galvanized coating exhibited the higher R_{cp} than the Cu pre-electrodeposited part after 1 h of immersion (Table III), since the passive state of galvanized coating is significantly associated with the formation of corrosion products ($\propto R_{cp}$). The utilization of a low potential scan rate of 0.5 $mV\ s^{-1}$ during the whole anodic polarization test could also account for the observed results. $Zn(OH)_2$ precipitates according to reactions 1 and 2.[37] During the open-circuit immersion in chloride-containing environment, $ZnCl_2\ 4Zn(OH)_2$ forms as a result of reaction 1 and accounts for the alkaline (pH 8–9) environment. This alkalinity might promote the stability of precipitates by the formation of $Zn(OH)_2$ over the galvanized coating (reaction 2). This passivity of galvanized coatings can be observed more clearly at -1.3–1.1 V_{SCE} after 4 days of immersion.

$$Zn + 5H_2O + 5/2O_2 + 2Cl^- \rightarrow ZnCl_2\ 4Zn(OH)_2 + 2OH^- \quad [1]$$

$$ZnCl_2\ 4Zn(OH)_2 + 2OH^- \rightarrow 5Zn(OH)_2 + 2Cl^- \quad [2]$$

The improvement in corrosion resistance of the Cu pre-electrodeposited galvanized coating clearly contrasts with the behavior of the conventional part after 4 days of immersion (Fig. 9b). As shown in Table III, the i_{corr} of conventional galvanized coating was sharply increased from 40.3 to 141.8 $\mu A\ cm^{-2}$ after 4 days of immersion, whereas this parameter remained nearly unchanged for the Cu pre-electrodeposited part. This result is also consistent with that of EIS analysis that the Cu pre-electrodeposited galvanized steel maintained almost constant R_p (rather increased) during 4 days of immersion (from 600.4 to 613.1 $\Omega\ cm^2$), which was decreased in the conventional part (from 258.6 to 174.7 $\Omega\ cm^2$). According to the mixed potential theory, this is directly produced by the decrease in the oxidation reaction rate of the Cu pre-electrodeposited galvanized coating since both coatings have approximately the same reduction reaction rate.

Conclusions

This study examined the effect of Cu pre-electrodeposits on the coating quality and the resultant corrosion characteristics of galvanized dual-phase steels. The crack and pin-hole type of coating defects were significantly reduced by pre-electrodepositing Cu, resulting in an increase in weight of galvanized coating. Further, the average spangle diameter was significantly decreased for this sample. This result suggests that the Cu pre-electrodeposits on the steel substrate could increase the solid/liquid interfacial energy, increasing the nucleation sites of new spangles in the solidifying Zn coatings during the galvanization. On the other hand, the Cu electrodeposits retarded the rate of Al uptake at the coating/substrate interface and fully disappeared after the galvanization, resulting in the development of the imperfect Fe-Al compounds. These phenomena indicate that the Cu electrodeposits act as a diffusion barrier between Fe and Al. However, the incubation time for the formation of Fe-Zn intermetallics during the galvanization seems to be increasing also by the Cu coating layer, leading to a decrease in coating defects. The Cu pre-electrodeposited galvanized coating afforded a higher corrosion resistance than conventional steels upon the immersion in an electrolyte. In particular, it effectively prevented the concentration polarization even after 4 days of immersion and acted as a barrier layer for steel surface. These results are directly owing to the decreased oxidation reaction rate of the Cu pre-electrodeposited galvanized coating since both galvanized coatings present similar reduction reaction rates.

Acknowledgment

This work was financially supported by the Ministry of Education, Science Technology (MEST) and National Research Foundation of Korea (NRF) through the Basic Research Laboratories (BRL) Program (2012-0000340).

References

1. "The role of Aluminum in continuous hot-dip galvanizing", <http://galvinfo.com/ginotes/GalvInfoNote_2_4.pdf> (2 July 2012).
2. "Galvannealed zinc-iron alloy coated steel", ArcelorMittal, <http://www.arcelormittal.com/automotive/saturnus/sheets/N_EN.pdf> (2 July 2012).
3. "Galvannealed – Difference from galvanize", GalvInfo, <http://galvinfo.com/ginotes/GalvInfoNote_1_3.pdf> (2 July 2012).
4. C. E. Jordan and A. R. Marder, *Metall. Mater. Trans. B*, **29**, 479 (1998).
5. M. Guttmann, *Mater. Sci. Forum*, **155**, 527 (1994).
6. M. Saito, Y. Uchida, T. Kittaka, Y. Hirose, and Y. Hisamatsu, *Tetsu-to-Hagane*, **77**, 947 (1991).
7. C. E. Jordan and A. R. Marder, *Metall. Mater. Trans. A*, **28A**, 2695 (1997).
8. A. Nishimoto, J. Inagaki, and K. Nakaoka, *Trans. ISIJ*, **26**, 807 (1986).
9. E. M. Bellhouse and J. R. McDermid, *Mater. Sci. Eng., A*, **491**, 39 (2008).
10. H. Liu, Y. He, S. Swaminathan, M. Rohwerder, and L. Li, *Surf. Coat. Tech.*, **206**, 1237 (2011).
11. I. Cvijović, I. Parezanović, and M. Spiegel, *Corros. Sci.*, **48**, 980 (2006).
12. E. M. Bellhouse and J. R. McDermid, *Metall. Mater. Trans. A*, **42**, 2753 (2011).
13. Y. F. Gong, H. S. Kim, and B. C. DeCooman, *ISIJ Int.*, **49**, 557 (2009).
14. S. Swaminathan, M. Rohwerder, and M. Spiegel, *Surf. Coat. Tech.*, **205**, 4089 (2011).
15. V. F. C. Lins, L. Madeira, J. M. C. Vilela, M. S. Andrade, V. T. L. Buono, J. P. Guimarães, and E. A. Alvarenga, *Appl. Surf. Sci.*, **257**, 5871 (2011).
16. X. S. Li, S. Baek, C. Oh, S. Kim, and Y. Kim, *Scripta Materialia*, **59**, 290 (2008).
17. S. Feliu Jr. and M. L. Pérez-Revenga, *Acta Materialia*, **53**, 2857 (2005).
18. A. van der Heiden, A. J. C. Burghardt, W. van Koesveld, E. B. van Perlstein, and M. G. J. Spanjers, in: A. R. Marder (Eds.): *The Physical Metallurgy of Zinc Coated Steel*, TMS, Warrendale, PA (1994) 251.
19. C. E. Jordan and A. R. Marder, *Metall. Mater. Trans. A*, **25**, 937 (1994).
20. www.posco.com.
21. Y. Tobiyama, C. Kato, N. Morito, and S. Umino, Japanese Patent Application No. PCT/JP/93/00394.
22. M. Sakurai, J. Inagaki, and T. Watanabe, Japanese Patent, Application No. JP-1994-088187.
23. R. Sa-nguanmoo, E. Nisaratanaporn, and Y. Boonyongmaneerat, *Corros. Sci.*, **53**, 122 (2011).
24. S. M. A. Shibli and R. Manu, *Surf. Coat. Tech.*, **197**, 103 (2005).
25. M. R. Yuan, J. T. Lu, G. Kong, and C. S. Che, *Surf. Coat. Tech.*, **205**, 4507 (2011).
26. B. Ramezanzadeh and M. M. Attar, *Surf. Coat. Tech.*, **205**, 4649 (2011).
27. S. L. Manchet, J. Landoulsi, C. Richard, and D. Verchère, *Surf. Coat. Tech.*, **205**, 475 (2010).
28. R. Berger, U. Bexell, T. M. Grehk, and S. E. Hörnström, *Surf. Coat. Tech.*, **202**, 391 (2007).
29. Y. I. Choi, W. J. Beom, C. J. Park, D. J. Paik, and M. H. Hong, *Metall. Mater. Trans. A*, **41**, 3379 (2010).
30. Y. I. Choi, E. S. Shin, K. Kkuroda, M. Okido, and C. J. Park, *Corros. Sci.*, **58**, 152 (2012).
31. "Selecting coating thickness (weight or mass) for galvanized steel sheet products", GalvInfo, <http://galvinfo.com/ginotes/GalvInfoNote_1_6.pdf>.
32. H. Leidheiser and D. K. Kim, *J. Metals*, 19 (Nov. 1976).
33. N. Y. Tang, *Met. Mater. Trans. A*, **26**, 1699 (1995).
34. M. Isobe, *CAMP-ISIJ*, **5**, 1629 (1992).
35. N. Perez, *Electrochemistry and Corrosion Science*, Springer, Boston, 140 (2004).
36. S. T. Vagge, V. S. Raja, and R. G. Narayanan, *Appl. Surf. Sci.*, **253**, 8415 (2007).
37. K. Hayashi and Y. Miyoshi, *Tetsu-to-Hagane*, **78**, 1577 (1992).